

Dynamically Spreading Frontal and Cingulate Deficits Mapped in Adolescents With Schizophrenia

Christine N. Vidal, PhD; Judith L. Rapoport, MD; Kiralee M. Hayashi, BS; Jennifer A. Geaga, BS; Yihong Sui, BS; Lauren E. McLemore, BS; Yasaman Alaghband; Jay N. Giedd, MD; Peter Gochman, MA; Jonathan Blumenthal, MA; Nitin Gogtay, MD; Rob Nicolson, MD; Arthur W. Toga, PhD; Paul M. Thompson, PhD

Context: We previously detected a dynamic wave of gray matter loss in childhood-onset schizophrenia that started in parietal association cortices and proceeded frontally to envelop dorsolateral prefrontal and temporal cortices, including superior temporal gyri.

Objective: To map gray matter loss rates across the medial hemispheric surface, including the cingulate and medial frontal cortex, in the same cohort studied previously.

Design: Five-year longitudinal study.

Setting: National Institute of Mental Health, Bethesda, Md.

Subjects: Twelve subjects with childhood-onset schizophrenia, 12 healthy controls, and 9 medication- and IQ-matched subjects with psychosis not otherwise specified.

Interventions: Three-dimensional magnetic resonance imaging at baseline and follow-up.

Main Outcome Measures: Gyral pattern and shape variations encoded by means of high-dimensional elastic deformation mappings driving each subject's cortical anatomy onto a group average; changes in cortical gray matter mapped by computing warping fields that matched sulcal patterns across hemispheres, subjects, and time.

Results: Selective, severe frontal gray matter loss occurred bilaterally in a dorsal-to-ventral pattern across the medial hemispheric surfaces in the schizophrenic subjects. A sharp boundary in the pattern of gray matter loss separated frontal regions and cingulate-limbic areas.

Conclusion: Frontal and limbic regions may not be equally vulnerable to gray matter attrition, which is consistent with the cognitive, metabolic, and functional vulnerability of the frontal cortices in schizophrenia.

Arch Gen Psychiatry. 2006;63:25-34

Author Affiliations: Laboratory of Neuro Imaging, Brain Mapping Division, Department of Neurology, David Geffen School of Medicine at UCLA, Los Angeles, Calif (Drs Vidal, Toga, and Thompson and Mss Hayashi, Geaga, Sui, McLemore, and Alaghband); and Child Psychiatry Branch, National Institute of Mental Health, National Institutes of Health, Bethesda, Md (Drs Rapoport, Giedd, Gogtay, and Nicolson and Messrs Gochman and Blumenthal).

SCHIZOPHRENIA IS A SEVERE AND debilitating neuropsychiatric disorder, with cognitive disturbances that include delusions, hallucinations, and psychosis. The cause of the disorder is unknown, but the study of severe, early-onset cases has disclosed a dynamic wave of cortical gray matter loss that spreads across the lateral surface of the brain as the disease progresses.¹ To relate this deficit trajectory to normal development and cognition, it is vital to determine whether brain systems are differentially affected. Neuroanatomic and imaging studies consistently describe frontal and cingulate deficits in patients with schizophrenia.²⁻⁵ No study, to our knowledge, has mapped how these deficits emerge or progress in early-onset cases. Using a new method, we mapped, for the first time, the transit of these deficits on the medial hemispheric surface, including key frontal and limbic regions implicated in schizophrenia.

Childhood-onset schizophrenia (COS)—in which psychotic symptoms occur by age 12 years—is a very rare form of the disorder that is neurobiologically continuous with the later-onset disorder.⁶⁻⁸ Adolescents with schizophrenia have a similar clinical presentation, with more severe premorbid symptoms and poorer prognosis.⁹⁻¹¹ Schizophrenia has been described as a neurodevelopmental disorder¹²⁻¹⁴ that may be triggered by excess cortical “pruning” during adolescence.¹⁵ However, the timing and dynamics of the cortical deficits are unknown.

In a previous study of COS,¹ we detected a dynamic wave of gray matter loss that started in parietal association cortices and proceeded frontally to envelop dorsolateral prefrontal and temporal cortices, including superior temporal gyri. In the present study, we used a new computational method to map gray matter loss rates across the medial hemispheric surface, including the cingulate and medial

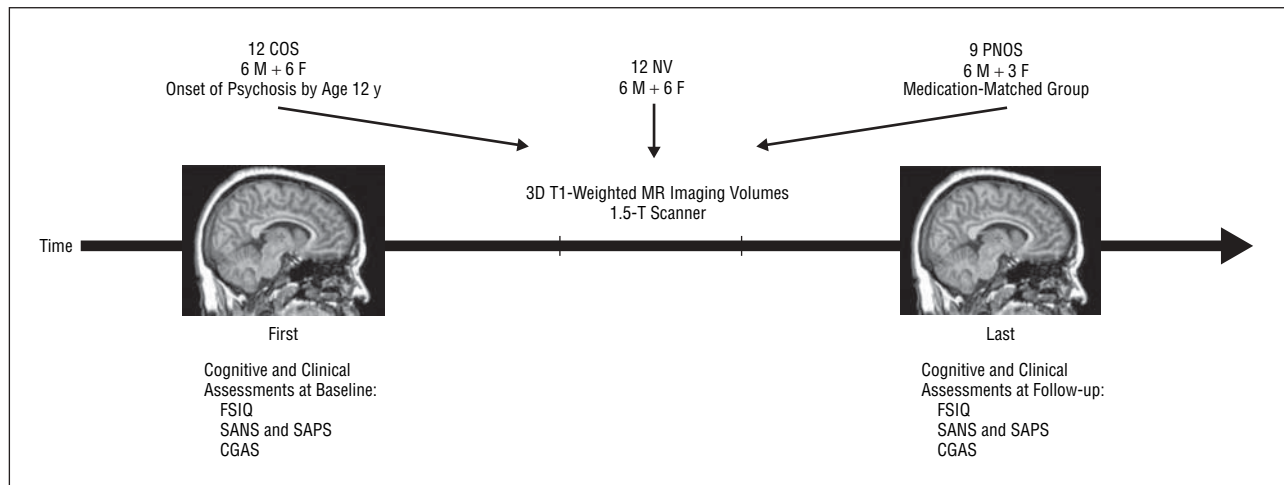


Figure 1. Subjects and magnetic resonance (MR) imaging. Subjects with childhood-onset schizophrenia (COS), normal volunteers (NV), and subjects with psychosis not otherwise specified (PNOS) were scanned twice, 5 years apart. When the baseline and follow-up scans were acquired, a cognitive and clinical evaluation was made, including the full-scale IQ (FSIQ), the Scale for Assessment of Positive Symptoms (SAPS), the Scale for Assessment of Negative Symptoms (SANS), and the Children's Global Assessment Scale (CGAS). Scores are reported in the Table and in the "Results" section. 3D indicates 3-dimensional.

frontal cortex, in the same cohort. The longitudinal design (5-year interval between images) tracks the disease as it evolves through the medial cortex, demonstrating the pattern of disease-specific loss. Our goal was also to link these deficits with cognitive and clinical assessments in the same subjects.

We expected to find an exaggerated pattern of medial frontal gray matter loss consistent with our previous findings of late dorsolateral prefrontal loss. We also expected correlations between medial cortical deficits and clinical and cognitive scores, and these were assessed by means of 4-dimensional maps. Finally, we studied sex effects and hemispheric asymmetry in these deficits, although these analyses were more exploratory.

METHODS

SUBJECTS

Twelve schizophrenic subjects (6 boys and 6 girls) and 12 healthy volunteers (6 boys and 6 girls), as well as 9 additional medication- and IQ-matched subjects (6 boys and 3 girls), were recruited as part of an ongoing National Institute of Mental Health (NIMH) study of COS.⁷ All subjects were studied prospectively during a 5-year period. All subjects with COS satisfied *DSM-III-R* diagnostic criteria for schizophrenia,¹⁶ with onset of psychotic symptoms by age 12 years (**Figure 1**). They all had a history of poor response to, or intolerance of, at least 2 atypical neuroleptics. They had a mean \pm SD full-scale IQ at study entry of 70.4 ± 12.9 and no other active neurologic disease or medical condition. Diagnosis was determined from clinical and structured interviews with the adolescents and their parents based on portions of the Schedule for Affective Disorders and Schizophrenia for School-Age Children—Epidemiologic Version¹⁷ and of the Diagnostic Interview for Children and Adolescents Revised,¹⁸ as well as from previous records. Psychopathologic symptoms were evaluated by means of the Scale for the Assessment of Positive Symptoms (SAPS),¹⁹ the Scale for the Assessment of Negative Symptoms (SANS),¹⁹ and the Children's Global Assessment Scale (CGAS).²⁰ Normal adolescents were screened for medical, neurologic, and psychiatric illness and learning disabilities.⁷ We matched the cohorts for age (**Table**), sex, follow-up interval

(which was identical), social background, and height. Medication and IQ effects were assessed by analyzing a second group of nonschizophrenic medication-matched subjects with psychosis not otherwise specified (PNOS). The 9 age- and sex-matched subjects with PNOS^{7,22} received the same medication as the schizophrenic group at baseline and were referred to NIMH with a diagnosis of COS, which was ruled out after a complete medication washout. They were also matched for IQ, age, and sex with the subjects with COS (mean \pm SD IQ, 76.0 ± 10.0), and matched for baseline age and sex with the healthy controls. These children had very transient psychotic symptoms, emotional lability, poor interpersonal skills, normal social interest, and multiple deficits in information processing.^{7,12,22} They were less severely impaired than the COS group but continued to have a mixture of mood and behavioral problems. None was schizophrenic at follow-up but rather exhibited chronic mood disturbance and lack of behavioral control; they were treated with both typical and atypical neuroleptics for these symptoms (at doses similar to those used for COS), which were quite effective in controlling the behaviors.

MAGNETIC RESONANCE IMAGING

Three-dimensional (3D) ($256^2 \times 124$ resolution) T1-weighted fast spoiled gradient echo magnetic resonance (MR) imaging volumes were acquired from all 33 subjects. All images were acquired on the same 1.5-T scanner (Signa; General Electric Co, Milwaukee, Wis) at the National Institutes of Health Clinical Center, Bethesda, Md. Imaging variables were as follows: time to echo, 5 milliseconds; time to repeat, 24 milliseconds; flip angle, 45° ; number of excitations, 1; and field of view, 24 cm. The same set of 12 healthy controls were scanned at baseline and after a 5-year interval (**Figure 1**; **Table** shows mean age). In parallel, the 12 age- and sex-matched schizophrenic subjects were identically scanned at the same ages and intervals.

IMAGE PROCESSING AND ANALYSIS

Images acquired across the multiyear time span were processed as follows. Briefly, for each scan pair, a radiofrequency bias field correction algorithm eliminated intensity drifts due to scanner field inhomogeneity. The initial scan was rigidly aligned (registered) to the target²³ and resampled with the use of chirp-Z (in-plane) and linear (out-of-plane) interpolation.

Table. Demographic and Clinical Characteristics and Medication Information for the COS, PNOS, and NV Groups*

Characteristics	Mean ± SD			t Statistic	P Value
	COS (n = 12)	PNOS (n = 9)	NV (n = 12)		
Baseline age, y	14.1 ± 2.7	13.6 ± 2.7	13.5 ± 2.4	0.4	.68 (COS, PNOS)
Follow-up age, y	18.7 ± 3.1	16.4 ± 2.3	18.0 ± 2.8	0.6	.54 (COS, NV)
				0.1	.90 (NV, PNOS)
				1.8	.08 (COS, PNOS)
Full-scale IQ at baseline†	68.0 ± 17.5	77.9 ± 12.8	123.9 ± 16.9	0.5	.61 (COS, NV)
Full-scale IQ at follow-up†	70.2 ± 14.6	77.0 ± 11.1	123.9 ± 16.9	1.4	.17 (NV, PNOS)
Clinical functioning at time 1‡				1.4	.18 (COS, PNOS)
SANS	73.7 ± 15.7	23.6 ± 21.0	NA	5.4	<.001
SAPS	58.2 ± 17.6	23.0 ± 23.2	NA	3.6	.002
CGAS	28.4 ± 10.8	52.0 ± 18.9	NA	3.3	.005
Clinical functioning at time 2‡					
SANS	49.8 ± 28.4	22.9 ± 19.2	NA	2.2	.04
SAPS	16.5 ± 10.3	11.8 ± 8.5	NA	1.0	.35
CGAS	42.4 ± 18.6	40.6 ± 15.1	NA	0.2	.83
Medication at baseline§					
Typical antipsychotics	854.5 ± 800.4	1793.9 ± 2650.1	NA	1.0	.33
Atypical antipsychotics	65.5 ± 50.2	5.0 ± 1.7	NA	2.0	.10
Mood stabilizers	800.0 ± 192.3	1310.0 ± 323.4	NA	1.0	.21
Antidepressants	NA	NA	NA	NA	NA
Medication at follow-up§					
Typical antipsychotics	502.0 ± 673.2	633.3 ± 665.8	NA	0.3	.81
Atypical antipsychotics	182.6 ± 112.1	94.8 ± 184.9	NA	1.1	.29
Mood stabilizers	2016.6 ± 772.1	1340.6 ± 198.9	NA	1.0	.35
Antidepressants	132.5 ± 70.9	150.0 ± 20.4	NA	0.2	.82

Abbreviations: CGAS, Children's Global Assessment Scale; COS, childhood-onset schizophrenia; NA, not applicable; NV, normal volunteers; PNOS, psychosis not otherwise specified; SANS, Scale for the Assessment of Negative Symptoms; SAPS, Scale for the Assessment of Positive Symptoms.

*Higher scores on the SANS and SAPS represent greater symptom severity, while higher scores on the CGAS represent better functioning.

†According to the Wechsler Intelligence Scale for Children or Wechsler Adult Intelligence Scale.

‡Comparison between COS and PNOS.

§Antipsychotics included thiothixene, clozapine, haloperidol, chlorpromazine hydrochloride, trazodone hydrochloride, olanzapine, thioridazine hydrochloride, risperidone, and mesoridazine besylate. Mood stabilizers included divalproex sodium, lithium carbonate, valproic acid, valproate sodium, carbamazepine, and gabapentin. Antidepressants included sertraline hydrochloride, clomipramine hydrochloride, imipramine hydrochloride, fluvoxamine maleate, and fluoxetine hydrochloride. Medication dosage is given in milligrams per day and is the dosage patients received for maintenance. Dosages for typical antipsychotics are reported in terms of chlorpromazine equivalents (milligrams per day) according to the formula proposed by Davis.²¹ Risperidone was considered atypical unless its dosage was above 6 mg/d (for more details regarding this formula and its definitions, see Davis²¹).

TISSUE MAPS

To equalize image intensities across subjects, registered scans had their intensity histograms matched. A supervised tissue classifier generated detailed maps of gray matter, white matter, and cerebrospinal fluid, as described in previous studies.^{24,25} The interrater and intrarater reliability of this protocol has been described previously.²⁵ Gray and white matter maps were retained for subsequent analysis.

3D CORTICAL MAPS

A surface model of the cortex was automatically extracted²⁶ for each subject and time point as described previously,¹ but modified to extract the interhemispheric (medial) cortical surface for both brain hemispheres, allowing cingulate and other limbic, frontal, parietal, occipital, and ventral cortices to be resolved, as well as the corpus callosum.²⁷ This software deforms a meshlike surface to fit a cortical surface tissue threshold intensity value from the brain volume. The intensity threshold was defined as the MR imaging signal value that best differentiated cortical cerebrospinal fluid on the outer surface of the brain from the underlying cortical gray matter.

CORTICAL PATTERN MATCHING

An image analysis technique known as *cortical pattern matching*²⁷ was used to localize disease effects on cortical anatomy over time and to increase the power to detect systematic group differences and changes. The approach models and controls for gyral pattern variations across subjects. It visualizes average maps of cortical change in a population and encodes its variance and any group differences. From each subject's cortical models at different time points, a 3D deformation vector field was computed measuring brain surface shape change across the time interval.¹ This accommodates any brain shape changes when cortical gray matter is compared within a subject across time. The deformation reconfigures the earlier cortex into the shape of the later one, matching the entire gyral patterns and cortical surfaces in the pair of 3D image sets.

Matching Cortical Anatomy Across Subjects

A second deformation was computed that matches gyral patterns across all the subjects in the study, in addition to the deformation that matches anatomy over time. This allows data to be averaged and compared across corresponding cortical re-

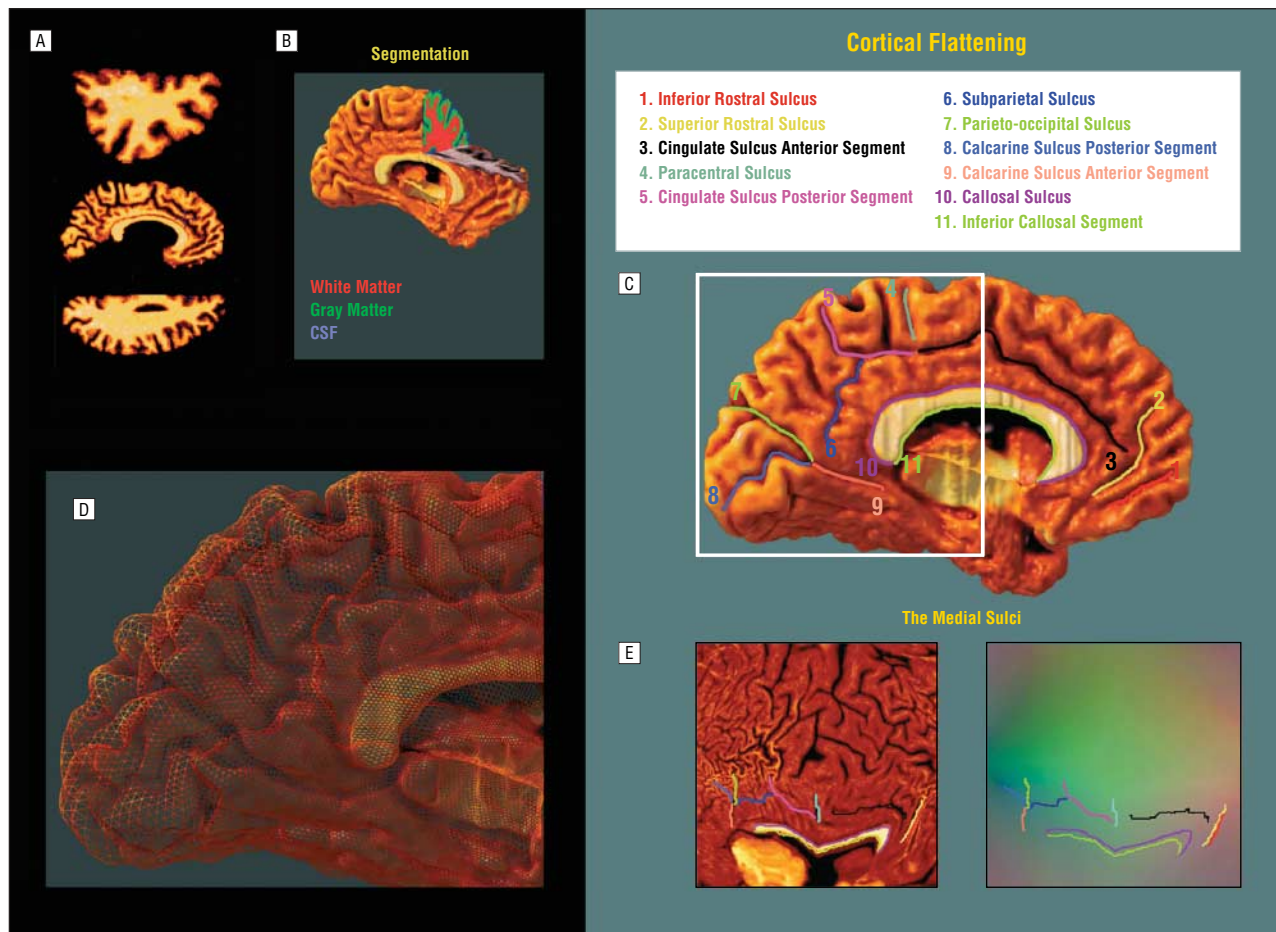


Figure 2. Demonstration of cortical flattening. Cortical flattening and sulcal matching are anatomic modeling steps used to help create 3-dimensional average cortical models and gray matter maps for subjects with childhood-onset schizophrenia and their matched controls. Each individual magnetic resonance image (A), after removal of nonbrain tissues, is segmented into gray matter, white matter, and cerebrospinal fluid (CSF) (B). A 3-dimensional cortical model is created for each subject, and 11 medial sulci and 7 reference lines are traced as 3-dimensional curves directly on this surface model (C). The surface is made up of discrete triangular tiles (D), and a geometric flattening process is applied to lay out the cortical regions, and the sulcal curves that delimit them, as features in 2 dimensions (E). Information on where these cortical points originally came from in 3 dimensions is preserved in this 2-dimensional image format: using a color-coding system, cortical points' 3-dimensional locations (x, y, z) are given unique colors, and these colors are plotted into the flat map (E).

gions (the algorithm for this is described in Thompson et al^{28,29}). A set of sulcal landmarks per brain is used to constrain the mapping of one cortex onto another. This associates corresponding cortical regions across subjects. An image analyst (C.N.V.), blind to subject diagnosis, sex, and age, traced each of 11 sulci in each hemisphere on the medial surface rendering of each subject's brain. Landmarks were defined according to a detailed anatomic protocol³⁰⁻³³ based on the *Atlas of the Cerebral Sulci*.³⁴ This protocol is available on the Internet³³ and has known interrater and intrarater reliability, reported previously.³²

Average Cortical Model Construction

To create an average 3D cortical model for each group of subjects, the following steps were used.¹ For each subject, all sulcal-gyral landmarks (**Figure 2C** and **E**) were flattened into a 2-dimensional plane along with the cortical model.³⁵ A color code (**Figure 2E**) retains the original 3D position of each cortical point as a red, green, and blue color triplet plotted in the 2-dimensional parameter space. Once data are in this flat space, sulcal features are aligned across subjects with a warping technique. Local measures of gray matter density were convected along with these warps and plotted on the average cortex before statistical analysis. Confounding effects of cross-subject anatomic variance are greatly reduced, empowering detection of disease effects.

Averaging Cortical Gray Matter Maps

A local measurement of gray matter density was made in each subject and averaged across equivalent cortical locations. To quantify local gray matter, we used a measure termed *gray matter density*, used in many previous studies to compare the spatial distribution of gray matter across subjects.^{1,25,27,36-39} This measures the proportion of gray matter in a small region of fixed radius (15 mm) around each cortical point. Given the large anatomic variability in some cortical regions, high-dimensional elastic matching of cortical patterns^{27,28} associated gray matter density measures from homologous cortical regions first across time and then also across subjects. This cortical matching localizes deficits relative to gyral landmarks; it also averages data from corresponding gyri, which is impossible if data are mapped only linearly into stereotaxic space. Annualized 4-dimensional maps of gray matter loss rates within each subject were elastically realigned for averaging and comparison across diagnostic groups.

MAPPING GRAY MATTER LOSS

Statistical maps were generated indicating locally the degree to which gray matter loss rates were statistically linked with diagnosis and clinical performance (CGAS, SANS, and SAPS

scores). To do this, at each cortical point, a multiple regression was run to assess whether the gray matter loss rate at that point depended on the covariate of interest (eg, test scores, diagnosis). The *P* value describing the significance of this linkage was plotted at each cortical point by means of a color code to produce a statistical map.

PERMUTATION TESTING

Maps identifying these linkages were assessed statistically by permutation. The presence of significant effects in statistical maps can be tested by Gaussian random field theory⁴⁰ or by non-parametric (eg, permutation) methods, both of which have been applied in functional⁴¹ and structural^{25,37} brain imaging. We used permutation to avoid making assumptions about the spatial covariance of the residuals⁴² (see Thompson et al^{28,29}). The total area of the average surface with suprathreshold statistics was used rather than the number of surface vertices with suprathreshold statistics because the total area is invariant to the sampling density of points on the surface.

RESULTS

RATE OF GRAY MATTER LOSS IN COS

Three-dimensional maps of brain changes, derived from the same subjects over time, showed profound, progressive gray matter loss in some medial wall regions in schizophrenia (**Figure 3A**). In schizophrenic subjects, a striking gray matter loss (peak values, >5% loss per year; pink colors in Figure 3A) was observed in superior medial frontal regions including the superior frontal and the precentral gyri. The cingulate gyrus was also progressively affected in the subjects with COS, an effect detected only in the left hemisphere. Also, the graph in Figure 3B shows a significant difference between subjects with COS and controls for loss rate in the left ($P < .02$) and right ($P < .01$) medial frontal cortex, and a significant difference in the left ($P < .047$) cingulate gyrus. The cingulate sulcus forms a sharp boundary between the severe gray matter loss in the medial frontal cortex and the subtler cingulate deficit. Normal adolescents showed subtle changes in the left and right superior medial frontal areas (left, 1.02% loss/y; right, 1.20% loss/y), as well as the right and left cingulate regions (left, 0.94% loss/y; right, 1.19% loss/y).

SIGNIFICANCE OF THE PROGRESSIVE LOSS

To understand whether these changes could be normal fluctuations, the variability in both the anatomic distribution and loss rates for gray matter were computed locally across the cortex and the significance of the changes was established. Again, schizophrenic subjects exhibited a significant gray matter loss, with progressive deficits throughout the superior medial frontal cortex (left, $P < .0092$; right, $P < .0067$, by permutation), including the superior frontal and precentral gyri. A subtraction map was created to emphasize the fundamental loss pattern specific to the disease. The cingulate sulcus stands out

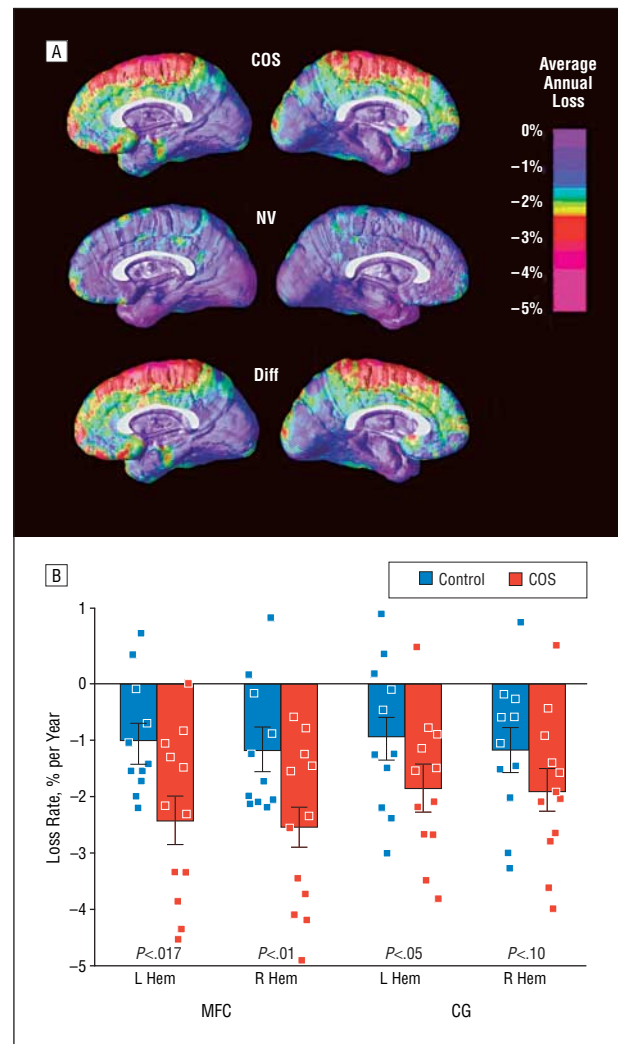


Figure 3. Average rate of gray matter loss in normal adolescents and schizophrenic subjects. A, The maps show the average local rates of loss for gray matter in the medial cortex of subjects with childhood-onset schizophrenia (COS) (top row), normal volunteer (NV) adolescents (middle row), and the difference (Diff) between both groups (bottom row). The superior medial frontal cortex exhibits the most strongly progressive deficits in the disease (left hemisphere, $P < .008$; right hemisphere, $P < .03$; 1-tailed *t* test). Progressive cingulate loss in the left hemisphere was observed in the group of adolescents with schizophrenia between 13 and 18 years of age when compared with the normal subjects ($P < .047$, 1-tailed *t* test). The color code shows the percentage of gray matter lost per year. B, We computed the average gray matter loss rate for the 24 subjects in the 2 anatomic areas of interest, the superior medial frontal cortex (MFC) and the cingulate gyrus (CG) in both left and right hemispheres (Hem). Error bars indicate the SE of the sample means, by region, in controls and subjects with COS. Individual loss rates as percentages per year are plotted, showing significant group separation for both right and left hemispheres in the frontal regions, and only on the left side for the cingulate areas.

as the anatomic boundary between the precipitous loss in medial frontal areas and the less affected limbic cortex. Maps of the significance of the dynamic gray matter loss in subjects with COS and normal adolescents are not presented, as they show patterns that are almost identical to those seen in Figure 3. They confirm a highly significant, progressive deficit localized primarily in the superior medial frontal cortex of the subjects with COS (Figure 3A, top row), with little loss in the medial wall in normal adolescents (Figure 3A, middle row).

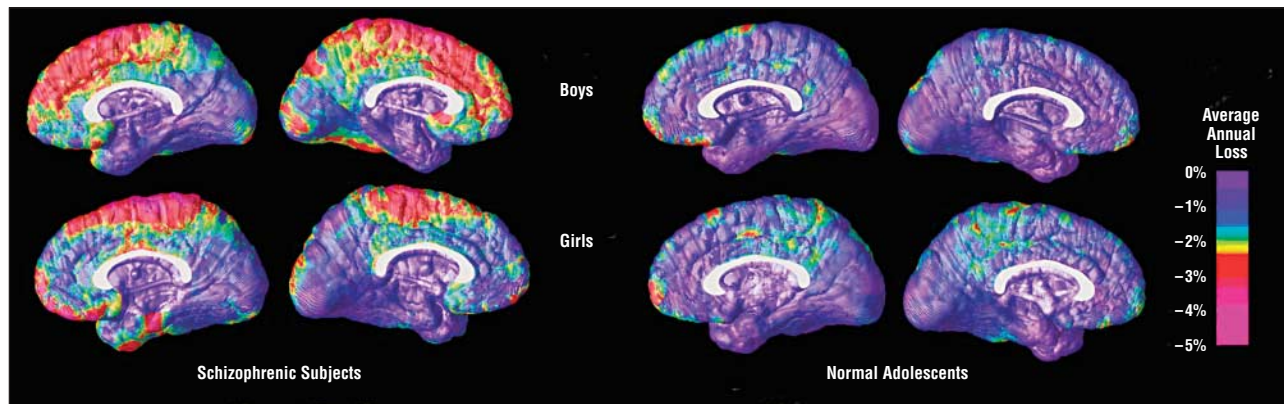


Figure 4. Dynamic changes of gray matter loss in boys and girls in both groups of schizophrenic subjects and normal adolescents. These maps show similar patterns of deficits for both sexes in both groups of subjects.

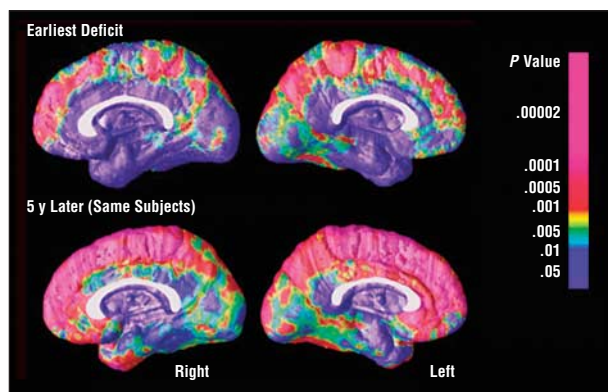


Figure 5. Mapping early and late deficits in schizophrenia. The maps here represent the deficits occurring during the development of schizophrenia, detected by comparing average profiles of gray matter between subjects with childhood-onset schizophrenia and controls at their first scan (age 13 years; top row) and their last scan 5 years later (age 18 years; bottom row).

SEX DIFFERENCES

Dynamic maps of gray matter loss were made for independent samples of male and female schizophrenic subjects and normal adolescents. Because some studies have found differences between male and female schizophrenic subjects in the severity or pattern of anatomic deficits, we assessed whether the findings were observed in both boys and girls. The same pattern of gray matter loss was identified in the 2 groups (**Figure 4**, left panels). Boys exhibited gray matter deficits in the superior frontal medial cortex (left, 2.15% loss/y; right, 2.02% loss/y), as did girls (right, 1.58% loss/y; left, 1.80% loss/y). The difference was not significant. A similar profile and degree of progressive gray matter loss may operate in COS, irrespective of sex.

SIGNIFICANCE OF EARLY AND LATE GRAY MATTER DEFICITS

Because the dynamic maps (Figure 3 and Figure 4) capture only loss that intensifies over time, we were concerned that earlier deficits may not have been detected in these progression maps. To detect earlier loss, we compared gray matter profiles across all 24 subjects at their first scan (**Figure 5**, top row) and at their last scan 4.6

years later (Figure 5, bottom row). The maps in Figure 5 show the significance of these effects. Medial frontal cortex was affected early in the disease from the anterior frontal regions to the posterior limit of the precentral gyrus in both right ($P < .019$) and left ($P < .031$) hemispheres. This deficit was stronger at follow-up in each hemisphere (left, $P < .0011$; right, $P < .0004$). The medial parietal cortex was also significantly affected early and late in the disease (baseline: left, $P < .023$; right, $P < .043$; follow-up: left, $P < .001$; right, $P < .021$). Importantly, the cingulate is relatively preserved at the onset of the disease, but is significantly affected at follow-up, in the left hemisphere ($P < .0078$). Frontal deficits, which are characteristic of adult and childhood schizophrenia, were severely progressive but still present in the early phase of the disease. The time course of these gray matter losses can be observed in video sequences (see supplementary data in video format, available at http://www.loni.ucla.edu/~thompson/chvidal/COS_MEDIAL/maps.html). These movies show the significant progression of gray matter loss in COS from the first scan (age 13 years) to the last scan (age 18 years).

MEDICATION EFFECTS

To determine whether neuroleptics had a role in the progressive gray matter deficit observed in our group of adolescents with COS, we assessed a medication-matched group. We performed mapping in 9 serially imaged subjects referred to the childhood schizophrenia study who did not meet diagnostic criteria for schizophrenia (labeled PNOS according to *DSM-III-R* terms).²² As seen in **Figure 6**, the nonschizophrenic group did show subtle but significant tissue loss, but this was much less marked than for the schizophrenic subjects. Intriguingly, the subjects with PNOS, who shared some of the deficit symptoms but did not satisfy criteria for schizophrenia, exhibited significantly accelerated gray matter loss in superior medial frontal and cingulate areas relative to healthy controls, in approximately the same, but a less pervasive, region than schizophrenics (left hemisphere: medial frontal cortex, $P < .050$; cingulate gyrus, $P < .022$). These findings suggest that the progression of the deficit in the medial frontal cortex is somewhat specific to schizophrenia regardless of medication.

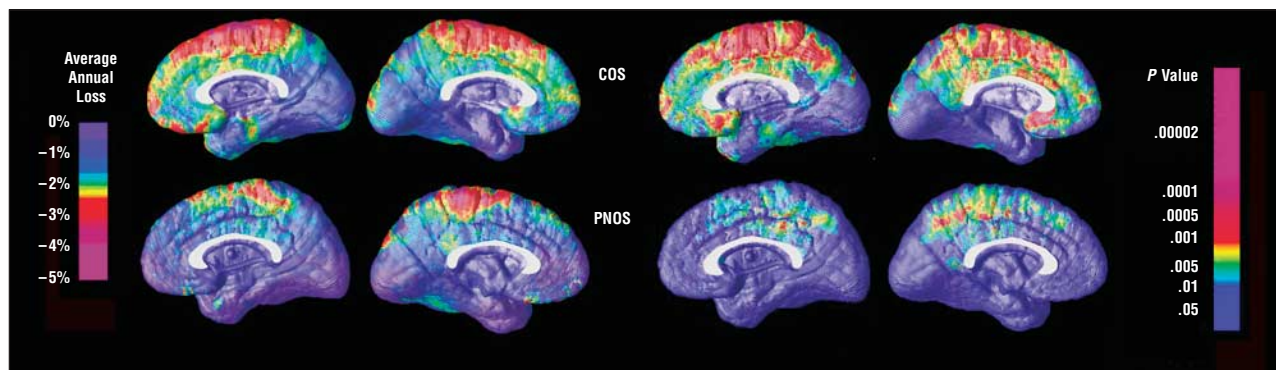


Figure 6. Average gray matter loss rates and maps of their significance in both adolescents with childhood-onset schizophrenia (COS) and psychosis not otherwise specified (PNOS). The same spatial pattern of loss is present in both groups but with a different degree of severity. The progressive gray matter loss found in the subjects with PNOS was significantly different from that in the COS group in the left hemisphere ($P < .03$, 1-tailed, after adjusting for sex).

CLINICAL AND COGNITIVE CORRELATES

Using clinical and cognitive evaluations made at the same time the scans were acquired, we established the relationship between these performances and gray matter loss. Scores on the clinical and cognitive evaluations are reported in the Table; they showed significant clinical improvement at follow-up, as measured by the SAPS, SANS, and CGAS. The mean \pm SD CGAS scores (higher scores represent better functioning) improved from 28.4 ± 10.8 at study entry to 42.4 ± 18.6 at follow-up ($P < .03$; Table) for the COS group. Measures at follow-up of parietal (right, $P < .006$; left, $P < .0048$; all P values corrected), frontal (right, $P < .018$; left, $P < .03$; all P values corrected), and cingulate (right, $P < .042$; left, $P < .021$; all P values corrected) cortex loss correlated strongly with CGAS total score at final scan (**Figure 7**, top row); perhaps surprisingly, better functioning was associated with higher gray matter density at follow-up. The amount of gray matter at follow-up in both occipital (right, $P < .009$; left, $P < .019$; all P values corrected) and parietal (right, $P < .011$; left, $P < .022$; all P values corrected) cortex (Figure 7, bottom row) was significantly associated with the clinical profile of positive symptoms (SAPS scores) at follow-up (eg, hallucinations or delusions; high scores represent greater illness). The mean \pm SD SAPS scores improved from 58.2 ± 17.6 at baseline to 16.5 ± 10.3 at follow-up ($P < .0001$). This correlation was such that lesser symptoms at follow-up were associated with less gray matter density. There was no significant correlation between negative symptoms (SANS; eg, flat affect, poverty of speech) and gray matter loss at either baseline or follow-up. However, the COS group showed an improvement as measured by the SANS, from 73.7 ± 15.7 to 49.8 ± 28.4 ($P = .02$). There was no significant correlation between gray matter loss and full-scale IQ, at either baseline or follow-up, and no significant change in full-scale IQ over time for any group. In summary, the clinical measures improved during the study, and the 2 test scores that linked with gray matter measures at follow-up were the CGAS and SAPS.

COMMENT

These longitudinal brain maps show that the medial frontal cortex is affected early in COS. Frontal atrophy is se-

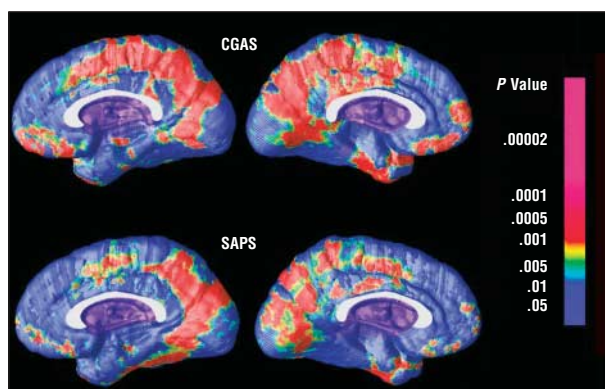


Figure 7. Maps of the correlation between gray matter deficits and cognitive and clinical performance. The upper maps represent the significance of the correlation between gray matter at follow-up and the Children's Global Assessment Scale (CGAS) at follow-up. The gray matter deficit in some parietal and occipital areas is significantly linked to the global assessment of function of adolescents with schizophrenia. The same deficits are also linked with scores on the Scale for Assessment of Positive Symptoms (SAPS), but to a lesser degree.

verely progressive and increases during a 5-year period in both brain hemispheres. The adjacent cingulate cortex is less severely affected at onset, but accelerated gray matter loss is observed later. Video sequences (see supplementary data) show that these deficits intensify in an apparent exaggeration of normal adolescent gray matter changes.^{15,42}

Notably, a sharp boundary in the profile of gray matter loss is visible between frontal and limbic tissue (Figure 3A), suggesting differential susceptibility. These findings are somewhat opposite to the sequence of cortical atrophy observed in Alzheimer disease,^{27,43} where the cingulate sulcus divides frontal areas that are relatively spared, and limbic regions with severe deficits early in the disease. Cortical atrophy may therefore differ sharply on either side of known architectonic and functional boundaries.

The PNOS group included in this study supports the notion that the large progressive changes seen in COS are not attributable purely to psychiatric illness per se, or to having a lower IQ. Although the gray matter changes are significantly less pronounced in the PNOS group, there were some changes in that group, which may be due to

an ongoing psychotic disease process. Effects of medications in contributing to or modulating these changes cannot be ruled out. Even so, the changes in the COS group are significantly greater in magnitude and more pervasive anatomically than those in the PNOS group, making it unlikely that they are attributable solely to antipsychotic treatment, as the PNOS and COS groups received comparable medications.

Clinical measures (including CGAS and SAPS scores) improved as the disease progressed and were found, in this study, to correlate with the degree of gray matter loss at follow-up in the medial frontal, medial parietal, and cingulate areas. Somewhat surprisingly, the associations we found between symptoms and gray matter measures were in an unexpected direction but were significant. In a previous study of a larger sample of patients with COS (N=39), Sporn et al⁴⁴ found an unexpected link between gray matter loss rates and percentage improvement on 2 scales: the Brief Psychiatric Rating Scale⁴⁵ and SANS scores. Perhaps because our sample size was small (N=12), we did not detect these correlations in the current sample, but there is some preliminary evidence that the gray matter amounts at follow-up are positively associated with SAPS scores, meaning that worse symptoms were linked with higher gray matter volume (when both measures were assessed at follow-up). This finding is paradoxical, as it is not explainable by differences in baseline symptom severity. There were no detected links between gray matter volumes and clinical scores at baseline; correlation was found with final scores only. We will investigate this correlation in larger samples to ascertain whether it is replicable; it is noteworthy that 2 other studies^{46,47} also found counterintuitive links between gray matter measures at follow-up and clinical measures. It remains possible that there is an ongoing process of brain structure deterioration that is not completely opposed by medication (if at all), even with measurable clinical improvement in response to treatment.

Full-scale IQ did not change significantly over time in any of the 3 subject groups. Perhaps surprisingly, there was no significant correlation between full-scale IQ and gray matter loss rates in any of the 3 groups, and IQ was not found to correlate with gray matter amounts at baseline or follow-up. There were significant IQ differences between the 2 psychiatric groups (COS and PNOS) and the healthy controls, which might be associated with some anatomic differences between the groups such as reduced gray matter at baseline in COS. In other studies, we and others found correlations between IQ and the overall volume of cortical gray matter,^{48,49} but these effects were weak positive correlations, and no correlation was observed with the longitudinal measures (loss rates) in any of the groups. We therefore did not control for IQ across the sample, as it is inextricably correlated with diagnosis and doing so would incorrectly eliminate some disease-specific effects. Within the groups of patients, however, gray matter variations or loss rates did not correlate with IQ. This does not rule out the possibility that an IQ effect may be detectable, in principle, if patients with COS could be assessed with a wider range of IQs.

The relationship between these measures may be more complex, but the changes seen in this study do not ap-

pear to be linked with IQ.⁵⁰ Nonetheless, the poor clinical and cognitive profiles, at onset, are consistent with the early cortical deficits observed in the medial frontal cortices.

The overall profile of progressive frontal gray matter loss reinforces the notion that COS is neurobiologically continuous with the later onset illness.⁷ Kuperberg et al⁵¹ found significant cortical thinning in the medial frontal areas of adult patients, and gray matter reductions have been reported in the medial premotor cortex,⁵² medial frontal gyri,^{2,53,54} and the medial prefrontal cortex.⁵⁵ Frontal gray matter reductions are even found in those at genetic risk for schizophrenia and in the prodromal phase of the illness,^{56,57} where they may relate to premorbid neuropsychological deficits in executive function.⁵⁷ Jacobsen et al⁵⁸ studied the Continuous Performance Test in a cohort of subjects with COS, a test that normally increases frontal metabolism. They found an increased metabolic rate in supramarginal gyrus and inferior frontal gyrus–insula but a decreased metabolic rate in middle frontal gyrus and superior frontal gyrus in COS. Functional MR imaging studies also showed reduced activation in medial frontal cortex of schizophrenic patients during the Tone Serial Position Task.⁵²

Frontal gray matter deficits may also be progressive in adults.⁵⁹ Some protective effect of atypical medications for progressive cortical loss has been observed in adult patients,⁶⁰ but almost all patients in this study were being treated with atypical medications, and there was still significant gray matter loss.

Although the medial frontal cortex is affected early and deteriorates later in the disease, the cingulate cortex is significantly affected only later in adolescence. Indeed, the anterior cingulate gyrus is involved in emotional and attentional functions,⁶¹ which are commonly reported to be altered in schizophrenia.⁶²⁻⁶⁴ To assess the possibility that these progressive brain changes were attributable to medication or IQ effects, a second group of medication- and IQ-matched subjects was evaluated. This group also lost gray matter, but in the left cingulate, this was slower than in the COS group. In a volumetric study, Gogtay et al⁶⁵ found significantly greater cortical gray matter loss in subjects with COS than their medication-matched controls, showing that the deficit was not attributable to medication.

The neuropathology of schizophrenia is unclear, and the cellular correlate of this cortical atrophy is unknown. Selemon and Goldman-Rakic⁶⁶ suggested that decreased cortical volume in schizophrenia represents a reduction in neuropil and neuronal size, rather than overt neuronal loss.⁶⁷ The emphasis on neuronal changes, rather than changes in other cell types, is supported by MR spectroscopic studies that repeatedly report frontal and temporal reductions in *N*-acetylaspartate, a metabolite that is relatively specific to neurons. Some postmortem studies report increased cell packing density in Brodmann areas 9 and 10 of schizophrenic patients,^{68,69} reflecting a decrease in the amount of neuropil. Some studies report a similar effect in Brodmann area 32, which is considered part of the cingulofrontal transition cortex,^{70,71} or the medial prefrontal cortex.^{72,73} In Golgi-stained material, Broadbelt et al⁷⁴ found a significant decrease in the number of

both primary (29%) and secondary (46%) basilar dendrites on layer V pyramidal neurons and similar, but less severe, reductions in layer III. Any such decrease in cingulate and frontal dendritic fields or the associated synaptic surface area might cause or exacerbate impairments in information processing. An opposing hypothesis, also consistent with our data, is that derailed cortical myelination may contribute to the apparent regression of gray matter in MR imaging data.⁷⁵ Changes in white matter tracts and functional connectivity may also ensue if there are aberrant cellular changes in the cortical regions they connect.

Establishing a dynamic map of schizophrenia progression may also have predictive value for those at risk. In a prospective study of healthy at-risk subjects, Pantelis et al⁵⁷ found that those who developed psychosis had less gray matter than those who did not, and they also showed a greater progressive reduction in cingulate, parahippocampal, fusiform, orbitofrontal, and cerebellar gray matter. In those who had not become psychotic, longitudinal changes were restricted to the cerebellum, suggesting that the deficit region may expand to the cerebrum around the time of disease onset and spread anteriorly as a marker of cognitive and clinical decline. To address this, a prospective study of full siblings of the patients with COS is in progress.

Submitted for Publication: June 23, 2004; final revision received April 26, 2005; accepted April 28, 2005.

Correspondence: Paul M. Thompson, PhD, Room 4238, Reed Neurological Research Center, Laboratory of Neuro Imaging, Department of Neurology, David Geffen School of Medicine at UCLA, 710 Westwood Plaza, Los Angeles, CA 90095-1769 (thompson@loni.ucla.edu).

Funding/Support: This work was supported by intramural funding from the National Institute of Mental Health (NIMH), Bethesda, Md; research grants from the National Center for Research Resources, Bethesda (P41 RR13642), the National Library of Medicine, Bethesda (LM/MH05639), National Institute of Neurological Disorders and Stroke and NIMH, Bethesda (NINDS/NIMH NS38753); and a Human Brain Project grant to the International Consortium for Brain Mapping, funded jointly by NIMH and the National Institute on Drug Abuse, Bethesda (P20 MH/DA52176). Algorithm development was also supported by the National Institute for Biomedical Imaging and Bioengineering and the National Institute for Research Resources, Bethesda (grants R21 EB01561 and R21 RR019771 to P.M.T.).

REFERENCES

- Thompson PM, Vidal C, Giedd JN, Gochman P, Blumenthal J, Nicolson R, Toga AW, Rapoport JL. Mapping adolescent brain change reveals dynamic wave of accelerated gray matter loss in very early-onset schizophrenia. *Proc Natl Acad Sci U S A*. 2001;98:11650-11655.
- Sigmundsson T, Suckling J, Maier M, Williams S, Bullmore E, Greenwood K, Fukuda R, Ron M, Toone B. Structural abnormalities in frontal, temporal, and limbic regions and interconnecting white matter tracts in schizophrenic patients with prominent negative symptoms. *Am J Psychiatry*. 2001;158:234-243.
- Suzuki M, Nohara S, Hagino H, Kurokawa K, Yotsutsuji T, Kawasaki Y, Takahashi T, Matsui M, Watanabe N, Seto H, Kurachi M. Regional changes in brain gray and white matter in patients with schizophrenia demonstrated with voxel-based analysis of MRI. *Schizophr Res*. 2002;55:41-54.
- Takahashi T, Kawasaki Y, Kurokawa K, Hagino H, Nohara S, Yamashita I, Nakamura K, Murata M, Matsui M, Suzuki M, Seto H, Kurachi M. Lack of normal structural asymmetry of the anterior cingulate gyrus in female patients with schizophrenia: a volumetric magnetic resonance imaging study. *Schizophr Res*. 2002;55:69-81.
- Yucel M, Stuart GW, Maruff P, Wood SJ, Savage GR, Smith DJ, Crowe SF, Copolov DL, Velakoulis D, Pantelis C. Paracingulate morphologic differences in males with established schizophrenia: a magnetic resonance imaging morphometric study. *Biol Psychiatry*. 2002;52:15-23.
- Frazier JA, Giedd JN, Hamburger SD, Albus KE, Kaysen D, Vaituzis AC, Rajapakse JC, Lenane MC, McKenna K, Jacobsen LK, Gordon CT, Breier A, Rapoport JL. Brain anatomic magnetic resonance imaging in childhood-onset schizophrenia. *Arch Gen Psychiatry*. 1996;53:617-624.
- Jacobsen LK, Rapoport JL. Research update: childhood-onset schizophrenia: implications of clinical and neurobiological research. *J Child Psychol Psychiatry*. 1998;39:101-113.
- Nicolson R, Rapoport JL. Childhood-onset schizophrenia: rare but worth studying. *Biol Psychiatry*. 1999;46:1418-1428.
- Russell AT. The clinical presentation of childhood-onset schizophrenia. *Schizophr Bull*. 1994;20:631-646.
- Alagband-Rad J, McKenna K, Gordon CT, Albus KE, Hamburger SD, Rumsey JM, Frazier JA, Lenane MC, Rapoport JL. Childhood-onset schizophrenia: the severity of premorbid course. *J Am Acad Child Adolesc Psychiatry*. 1995;34:1273-1283.
- Gordon CT, Frazier JA, McKenna K, Giedd J, Zemetkin A, Zahn T, Hommer D, Hong W, Kaysen D, Albus KE. Childhood-onset schizophrenia: an NIMH study in progress. *Schizophr Bull*. 1994;20:697-712.
- Weiberger DR. Schizophrenia as a neurodevelopmental disorder: a review of the concept. In: Hirsch SR, Weinberger DR, eds. *Schizophrenia*. London, England: Blackwood Press; 1995:294-323.
- Bullmore ET, Frangou S, Murray RM. The dysplastic net hypothesis: an integration of developmental and dysconnectivity theories of schizophrenia. *Schizophr Res*. 1997;28:143-156.
- Cannon M, Caspi A, Moffitt TE, Harrington H, Taylor A, Murray RM, Poulton R. Evidence for early-childhood, pan-developmental impairment specific to schizophreniform disorder: results from a longitudinal birth cohort. *Arch Gen Psychiatry*. 2002;59:449-456.
- Feinberg I. Schizophrenia: caused by a fault in programmed synaptic elimination during adolescence? *J Psychiatr Res*. 1982;17:319-334.
- American Psychiatric Association. *Diagnostic and Statistical Manual of Mental Disorders, Revised Third Edition*. Washington, DC: American Psychiatric Association; 1987.
- Puig-Antich J, Orvaschel H, Tabrizi MA, Chambers W. *Schedule of Affective Disorders and Schizophrenia for School-Age Children—Epidemiologic Version*. New York, NY: New York State Psychiatric Institution and Yale University School of Medicine; 1980.
- Reich W, Welner Z, Herjanic B. *Diagnostic Interview for Children and Adolescents—Revised—Computer Program: Child/Adolescent Version and Parent Version*. North Tonawanda, NY: Multi-Health Systems; 1990.
- Andreasen NC. *Scale for the Assessment of Positive Symptoms (SAPS) and Scale for the Assessment of Negative Symptoms (SANS)*. Iowa City: Dept of Psychiatry, University of Iowa College of Medicine; 1983.
- Shaffer D, Gould MS, Brasic J. A children's global assessment scale (CGAS). *Arch Gen Psychiatry*. 1983;40:1228-1231.
- Davis JM. Dose equivalence of the antipsychotic drugs. *J Psychiatr Res*. 1974;11:65-69.
- Kumra S, Briguglio C, Lenane M. Including children and adolescents with schizophrenia in medication-free research. *Am J Psychiatry*. 1999;156:1065-1068.
- Woods RP, Cherry SR, Mazziotta JC. Rapid automated algorithm for aligning and reslicing PET images. *J Comput Assist Tomogr*. 1992;16:620-633.
- Zijdenbos AP, Dawant BM. Brain segmentation and white matter lesion detection in MR images. *Crit Rev Biomed Eng*. 1994;22:401-465.
- Sowell ER, Thompson PM, Holmes CJ, Jernigan TL, Toga AW. In vivo evidence for post-adolescent brain maturation in frontal and striatal regions. *Nat Neurosci*. 1999;2:859-861.
- MacDonald D, Kabani N, Avis D, Evans AC. Automated 3-D extraction of inner and outer surfaces of cerebral cortex from MRI. *Neuroimage*. 2000;12:340-356.
- Thompson PM, Hayashi KM, de Zubicaray G. Dynamics of gray matter loss in Alzheimer's disease. *J Neurosci*. 2003;23:994-1005.
- Thompson PM, Woods RP, Mega MS, Toga AW. Mathematical/computational challenges in creating deformable and probabilistic atlases of the human brain. *Hum Brain Mapp*. 2000;9:81-92.
- Thompson PM, Mega MS, Narr KL, Sowell ER, Blanton RE, Toga AW. Brain im-

- age analysis and atlas construction. In: Fitzpatrick M, ed. *Handbook of Medical Image Processing and Analysis*. Bellingham, Wash: SPIE Press; 2000:4-41.
30. Steinmetz H, Furst G, Freund HJ. Variation of perisylvian and calcarine anatomic landmarks within stereotaxic proportional coordinates. *AJNR Am J Neuroradiol*. 1990;11:1123-1130.
 31. Leonard CM. Structural variation in the developing and mature cerebral cortex: noise or signal? In: Thatcher RW, Reid Lyon G, Rumsey J, Krasnegor N, eds. *Developmental Neuroimaging: Mapping the Development of Brain and Behavior*. New York, NY: Academic Press; 1996:207-231.
 32. Sowell ER, Delis D, Stiles J, Jernigan TL. Improved memory functioning and frontal lobe maturation between childhood and adolescence: a structural MRI study. *J Int Neuropsychol Soc*. 2001;7:312-322.
 33. Hayashi KM, Thompson PM, Mega MS, Zoumalan CI. Medial hemispheric surface gyral pattern delineation in 3D: surface curve protocol. Available at: http://www.loni.ucla.edu/~khayashi/Public/medial_surface/MedialLineProtocol.htm. Accessed November 4, 2005.
 34. Ono M. *Atlas of the Cerebral Sulci*. Stuttgart, Germany: Thieme Verlag; 1990.
 35. Thompson PM, Mega MS, Woods RP, Zoumalan CI, Lindshield CJ, Blanton RE, Moussai J, Holmes CJ, Cummings JL, Toga AW. Cortical change in Alzheimer's disease detected with a disease-specific population-based brain atlas. *Cereb Cortex*. 2001;11:1-16.
 36. Wright IC, McGuire PK, Poline JB, Travers JM, Murray RM, Frith CD, Frackowiak RS, Friston KJ. A voxel-based method for the statistical analysis of gray and white matter density applied to schizophrenia. *Neuroimage*. 1995;2:244-252.
 37. Bullmore ET, Suckling J, Overmeyer S, Rabe-Hesketh S, Taylor E, Brammer MJ. Global, voxel, and cluster tests, by theory and permutation, for a difference between two groups of structural MR images of the brain. *IEEE Trans Med Imaging*. 1999;18:32-42.
 38. Ashburner J, Friston KJ. Voxel-based morphometry—the methods. *Neuroimage*. 2000;11:805-821.
 39. Good CD, Johnsrude IS, Ashburner J, Henson RN, Friston KJ, Frackowiak RS. A voxel-based morphometric study of ageing in 465 normal adult human brains. *Neuroimage*. 2001;14:21-36.
 40. Friston KJ. Theoretical neurobiology and schizophrenia. *Br Med Bull*. 1996;52:644-655.
 41. Holmes AP, Blair RC, Watson JD, Ford I. Nonparametric analysis of statistic images from functional mapping experiments. *J Cereb Blood Flow Metab*. 1996;16:7-22.
 42. Nichols TE, Holmes AP. Nonparametric permutation tests for functional neuroimaging: a primer with examples. *Hum Brain Mapp*. 2002;15:1-25.
 43. Gogtay N, Sporn A, Clasen LS, Greenstein D, Giedd JN, Lenane M, Gochman PA, Zijdenbos A, Rapoport JL. Structural brain MRI abnormalities in healthy siblings of patients with childhood-onset schizophrenia. *Am J Psychiatry*. 2003;160:569-571.
 44. Sporn AL, Greenstein DK, Gogtay N, Jeffries NO, Lenane M, Gochman P, Clasen LS, Blumenthal J, Giedd JN, Rapoport JL. Progressive brain volume loss during adolescence in childhood-onset schizophrenia. *Am J Psychiatry*. 2003;160:2181-2189.
 45. Overall JE, Gorham DR. The Brief Psychiatry Rating Scale. *Psychol Rep*. 1962;10:799-812.
 46. Gur RE, Cowell P, Turetsky BI, Gallacher F, Cannon T, Bilker W, Gur RC. A follow-up magnetic resonance imaging study of schizophrenia: relationship of neuroanatomical changes to clinical and neurobehavioral measures. *Arch Gen Psychiatry*. 1998;55:145-152.
 47. DeLisi LE, Sakuma M, Ge S, Kushner M. Association of brain structural change with the heterogeneous course of schizophrenia from early childhood through five years subsequent to a first hospitalization. *Psychiatry Res*. 1998;84:75-88.
 48. Thompson PM, Cannon TD, Narr KL, van Erp T, Poutanen VP, Huttunen M, Lonnqvist J, Standerskjold-Nordenstam CG, Kaprio J, Khaledy M, Dail R, Zoumalan CI, Toga AW. Genetic influences on brain structure. *Nat Neurosci*. 2001;4:1253-1258.
 49. Haier RJ, Jung RE, Yeo RA, Head K, Alkire MT. Structural brain variation and general intelligence. *Neuroimage*. 2004;23:425-433.
 50. Braak H, Braak E. Staging of Alzheimer-related cortical destruction. *Int Psychogeriatr*. 1997;9(suppl 1):257-261.
 51. Kuperberg GR, Broome MR, McGuire PK, David AS, Eddy M, Ozawa F, Goff D, West WC, Williams SC, van der Kouwe AJ, Salat DH, Dale AM, Fischl B. Regionally localized thinning of the cerebral cortex in schizophrenia. *Arch Gen Psychiatry*. 2003;60:878-888.
 52. Honey GD, Sharma T, Suckling J, Giampietro V, Soni W, Williams SC, Bullmore ET. The functional neuroanatomy of schizophrenic subsyndromes. *Psychol Med*. 2003;33:1007-1018.
 53. Paillere-Martinot M, Caclin A, Artiges E, Poline JB, Joliot M, Mallet L, Recasens C, Attar-Levy D, Martinot JL. Cerebral gray and white matter reductions and clinical correlates in patients with early onset schizophrenia. *Schizophr Res*. 2001;50:19-26.
 54. Stevens AA, Goldman-Rakic PS, Gore JC, Fulbright RK, Wexler BE. Cortical dysfunction in schizophrenia during auditory word and tone working memory demonstrated by functional magnetic resonance imaging. *Arch Gen Psychiatry*. 1998;55:1097-1103.
 55. Ananth H, Popescu I, Critchley HD, Good CD, Frackowiak RS, Dolan RJ. Cortical and subcortical gray matter abnormalities in schizophrenia determined through structural magnetic resonance imaging with optimized volumetric voxel-based morphometry. *Am J Psychiatry*. 2002;159:1497-1505.
 56. Cannon TD, Thompson PM, van Erp TG, Toga AW, Poutanen VP, Huttunen M, Lonnqvist J, Standerskjold-Nordenstam CG, Narr KL, Khaledy M, Zoumalan CI, Dail R, Kaprio J. Cortex mapping reveals regionally specific patterns of genetic and disease-specific gray-matter deficits in twins discordant for schizophrenia. *Proc Natl Acad Sci U S A*. 2002;99:3228-3233.
 57. Pantelis C, Velakoulis D, McGorry PD. Neuroanatomical abnormalities before and after onset of psychosis: a cross-sectional and longitudinal MRI comparison. *Lancet*. 2003;361:281-288.
 58. Jacobsen LK, Hamburger SD, Van Horn JD, Vaituzis AC, McKenna K, Frazier JA, Gordon CT, Lenane MC, Rapoport JL, Zimetkin AJ. Cerebral glucose metabolism in childhood onset schizophrenia. *Psychiatry Res*. 1997;75:131-144.
 59. Mathalon DH, Sullivan EV, Lim KO, Pfefferbaum A. Progressive brain volume changes and the clinical course of schizophrenia in men: a longitudinal magnetic resonance imaging study. *Arch Gen Psychiatry*. 2001;58:148-157.
 60. Lieberman JA, Phillips M, Gu H, Stroup S, Zhang P, Kong L, Ji Z, Koch G, Hamer RM. Atypical and conventional antipsychotic drugs in treatment-naive first-episode schizophrenia: a 52-week randomized trial of clozapine vs chlorpromazine. *Neuropsychopharmacology*. 2003;28:995-1003.
 61. Devinsky O, Morrell MJ, Vogt BA. Contributions of anterior cingulate cortex to behaviour. *Brain*. 1995;118:279-306.
 62. Cullum CM, Harris JG, Waldo MC, Smerhoff E, Madison A, Nagamoto HT, Griffith J, Adler LE, Freedman R. Neuropsychological and neuropsychological evidence for attentional dysfunction in schizophrenia. *Schizophr Res*. 1993;10:131-141.
 63. Harvey SA, Nelson E, Haller JW, Early TS. Lateralized attentional abnormality in schizophrenia is correlated with severity of symptoms. *Biol Psychiatry*. 1993;33:93-99.
 64. Carter CS, Mintun M, Nichols T, Cohen JD. Anterior cingulate gyrus dysfunction and selective attention deficits in schizophrenia: [15O]H₂O PET study during single-trial Stroop task performance. *Am J Psychiatry*. 1997;154:1670-1675.
 65. Gogtay N, Sporn A, Clasen LS, Nugent TF III, Greenstein D, Nicolson R, Giedd JN, Lenane M, Gochman P, Evans A, Rapoport JL. Comparison of progressive cortical gray matter loss in childhood-onset schizophrenia with that in childhood-onset atypical psychoses. *Arch Gen Psychiatry*. 2004;61:17-22.
 66. Selemon LD, Goldman-Rakic PS. The reduced neuropil hypothesis: a circuit based model of schizophrenia. *Biol Psychiatry*. 1999;45:17-25.
 67. Harrison PJ. The neuropathology of schizophrenia: a critical review of the data and their interpretation. *Brain*. 1999;122:593-624.
 68. Benes FM, McSparren J, Bird ED, SanGiovanni JP, Vincent SL. Deficits in small interneurons in prefrontal and cingulate cortices of schizophrenic and schizoaffective patients. *Arch Gen Psychiatry*. 1991;48:996-1001.
 69. Selemon LD, Rajkowska G, Goldman-Rakic PS. Abnormally high neuronal density in the schizophrenic cortex: a morphometric analysis of prefrontal area 9 and occipital area 17. *Arch Gen Psychiatry*. 1995;52:805-820.
 70. Vogt BA, Nimchinsky EA, Vogt LJ, Hof PR. Human cingulate cortex: surface features, flat maps, and cytoarchitecture. *J Comp Neurol*. 1995;359:490-506.
 71. Conti F, Barbarelli P, Melone M, Ducati A. Neuronal and glial localization of NR1 and NR2A/B subunits of the NMDA receptor in the human cerebral cortex. *Cereb Cortex*. 1999;9:110-120.
 72. Bachevalier J, Meunier M, Lu MX, Ungerleider LG. Thalamic and temporal cortex input to medial prefrontal cortex in rhesus monkeys. *Exp Brain Res*. 1997;115:430-444.
 73. Dombrowski SM, Hilgetag CC, Barbas H. Quantitative architecture distinguishes prefrontal cortical systems in the rhesus monkey. *Cereb Cortex*. 2001;11:975-988.
 74. Broadbelt K, Byne W, Jones LB. Evidence for a decrease in basilar dendrites of pyramidal cells in schizophrenic medial prefrontal cortex. *Schizophr Res*. 2002;58:75-81.
 75. Bartzokis G, Nuechterlein KH, Lu PH, Gitlin M, Rogers S, Mintz J. Dysregulated brain development in adult men with schizophrenia: a magnetic resonance imaging study. *Biol Psychiatry*. 2003;53:412-421.